Measurement of London penetration depth from holographic images of superconducting vortices: The influence of specimen thickness

J. Bonevich
National Institute of Standards and Technology, Metallurgy Division, Gaithersburg, Maryland 20899

D. Capacci
Department of Physics and Istituto Nazionale di Fisica per la Materia, viale B. Pichat 6/2, 40127 Bologna, Italy

K. Harada, H. Kasai, and T. Matsuda
Advanced Research Laboratory, Hitachi Ltd., Hatoyama-machi, Saitama-ken 350-03, Japan

R. Patti and G. Pozzi
Department of Physics and Istituto Nazionale di Fisica per la Materia, viale B. Pichat 6/2, 40127 Bologna, Italy

A. Tonomura
Advanced Research Laboratory, Hitachi Ltd., Hatoyama-machi, Saitama-ken 350-03, Japan
(Received 2 April 1997; revised manuscript received 4 August 1997)

High-resolution holographic data of superconducting vortices are presented and analyzed in order to extract a measurement of the London penetration depth by fitting the reconstructed phase across the core using an analytical one-dimensional London model. The resulting value of 50 ± 5 nm for the London penetration depth is obtained, which is about two times larger than the commonly accepted value of 30 nm used in previous simulations. It is shown that this discrepancy can be removed by taking into account the influence on the phase shift of the specimen thickness and of the associated broadening of the field lines near the surface. These results highlight the importance of the assumed model in order to extract from the analysis of experimental data reliable quantitative estimates of critical parameters such as the London penetration depth. [S0163-1829(98)04702-X]

INTRODUCTION

The successful observation of superconducting flux lines (fluxons) in thin specimens both in conventional and high-T_c superconductors by means of Lorentz microscopy[1–3] and electron holography[4] has required two basic ingredients: on one hand the technological development of the instrumentation, stimulated also by the introduction in electron microscopy of interferometry[5] and holography methods,[6,7] and on the other hand a better comprehension of the contrast mechanisms when nonconventional setups are investigated, e.g., when the thin specimen is not perpendicular but tilted with respect to the electron beam.[8]

The initial theoretical approach has been to model the fluxon as a bundle of straight flux tubes perpendicular to the specimen surface, where the electron optical phase shift for a single flux tube has an analytical form.[2,8] The magnetic flux distribution is given by the London model[9] corresponding to a flux line having an infinitely small normal core. In addition to being described by an analytical expression, this model has the advantage that a single parameter, the London penetration depth λ_L, completely characterizes the superconducting fluxon.

In our previous simulations[2] we used the most commonly quoted bulk value for λ_L of 30 nm. The obtained results have shown that the most relevant features of the experimental data are well interpreted by our model, apart from a difference between the theoretical and experimental defocus distances. More precisely, our model predicts that the out-of-focus contrast of the bright-dark globules associated with the fluxon will saturate at a definite image defocus. This defocus represents the best operating condition for the observations, as it is a trade-off between high image contrast and radius, related to the localization of the fluxon. At 300 kV this defocus distance is roughly given by $2000\,\mathrm{nm}^{-1}\ \lambda_L^2$,[3] but a more general relation can be drawn from one-dimensional modeling of the fluxon[10] obtaining $\lambda Z/\lambda_L^2 \simeq 8$, where Z is the defocus distance and λ the electron wavelength. The assumed value of 30 nm gives a defocus distance of about 2 mm, an order of magnitude lower than the experimental value of 20 mm currently used in the out-of-focus observations of niobium.

In order to better understand the origin of this discrepancy, we have extended our theoretical considerations to include the flux core topography proposed by Clem.[9,11,12] This topography removes the unphysical limitation of the infinitely small normal core and has the advantage of being described by an analytical expression depending on two parameters [the London length and the core radius ξ_c, linked to and of the same order of magnitude as the coherence length, ξ (Ref. 11)]. Nonetheless, simulations with this improved and physically more appealing model show that in both the Lorentz and holographic cases the predictions of the two models are very similar[10,13] and that the broadening of the field topography taken into account by the Clem bulk model does not explain the discrepancy.

Electron holography experiments are better suited to understanding this problem, as they are able to map directly the phase shift associated with the fluxon. However, previous observations[4] carried out with a large interference distance and field of view suffered from the drawback that the holographic point resolution ranged between 60 and 90 nm, a value which could substantially influence the analysis and interpretation of the experimental results. Therefore, high-resolution holography experiments[14] have been recently carried out.

Our aim here is to conduct a quantitative analysis of the obtained results: in particular, by fitting the reconstructed phase across the core by means of an analytical one-dimensional London model according to the findings of Ref. 10, it is possible to extract a value for the London penetration depth. The measured penetration depth is found to be larger than the commonly accepted value, however, it is in good agreement with the out-of-focus observations. The influence of the hologram point resolution on the fitting procedure is also discussed on the basis of one-dimensional simulations. It turns out that, unexpectedly, the error associated with the penetration depth is considerably lower than the point resolution. Provided that the resolution is better than the London penetration depth, the trend of phase is only negligibly affected by the spatial frequency filtering of reconstruction procedure.

These results have prompted us to reconsider the assumption that the fluxon is described by a bundle of straight flux tubes with a topography given by the London (or Clem) bulk model. Instead, relying on an analytical approximate solution of the Ginzburg-Landau equations in a thin film proposed by Clem,[15] we show that the broadening and bending of the field lines near the surface due to the finite specimen thickness can account for the observed discrepancy. This fact highlights the importance of model assumptions when interpreting the experimental data to obtain reliable measurements of critical parameters like the London penetration depth.

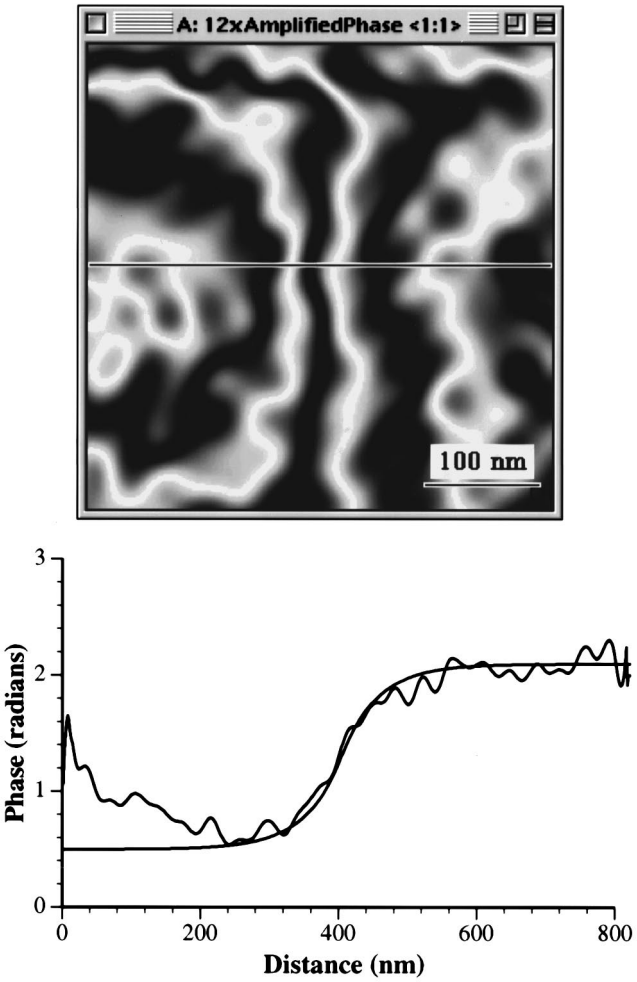

FIG. 1. A single fluxon as reconstructed in a 12× phase amplified interference micrograph (a). The phase profile across the fluxon core can be fit with a London parameter of 50 nm, larger than the bulk value of 30 nm (b). The phase difference across the fluxon is 0.5π and is affected on the left by bend contours in the foil.

EXPERIMENTAL RESULTS AND ANALYSIS

Our experiments were conducted as follows. First, cold-rolled and annealed Nb specimens were prepared by chemical polishing to final thicknesses of about 70 nm. These electron transparent foils were then sandwiched between two copper grids and inserted in a field-emission electron microscope equipped with a specially constructed low-temperature (liquid helium) magnetizing stage, allowing observations from 4.5 to 26 K in transverse magnetic fields up to 150 G.

The field emission gun, at 300 kV accelerating voltage, provided highly coherent and penetrating illumination and a rotatable electron biprism was used to form both low- and high-resolution holograms. Low-resolution conditions were formed by turning off the objective lens and focusing with the first intermediate lens. These holograms had carrier fringes of 30 nm spacing referred back to the specimen over a 4 μm width. High-resolution holograms were achieved by using the objective lens and had a fringe spacing down to 7 nm over a width of 1.5 μm.

While high-resolution holograms can give detailed phase information about the vortices, the reduced interference width limits the field of view and bend contours, present near the specimen edge, can affect the phase reconstructions. Furthermore, the comparison wave used to reconstruct high-resolution holograms must compensate for the nonplanar reference wave, requiring numerical fitting of the phase.

Figure 1(a) reports the reconstructed interference micrograph of a single fluxon with the phase amplified 12×. The vortex phase differences were evaluated by adding a linear tilt to the reconstructed phase map, thereby making the vortices appear as phase steps. The height of the step indicates the flux quantum, and the width can be taken to indicate the vortex diameter. While an infinitesimal flux tube appears as an abrupt phase step, real vortices with physical dimensions have smoothly sloped phase steps.

In order to quantitatively evaluate high-resolution holographic images, we can use the results of a recent paper.[10] This work showed that if the fluxon is modeled by a bundle of straight flux tubes with a field topography given by the bulk London or Clem models, then line scans of the phase across the fluxon center can be satisfactorily fitted by means of simple one-dimensional London or Clem models. Also, the problem of discriminating between the two models on the

basis of the experimental data alone has been addressed with the conclusion that: (i) differences between the curves representing the phase are not detectable as they are smaller than the experimental error, and (ii) discrimination could be performed by looking at the derivatives of the experimentally reconstructed phase.

On the basis of these results, we may address the problem of fitting the phase by limiting our attention to the simpler London model, described by the analytical expression

$$\varphi_L(x)=\mathrm{sign}(x)\,\frac{\Delta}{2}\left[1-\exp\left(-\frac{|x|}{\lambda_L^*}\right)\right], \tag{1}$$

where Δ is the maximum phase difference and λ_L^* is a parameter dependent on, and of the same order of magnitude as, the London penetration depth.

The experimental phase profile across the fluxon core is shown in Fig. 1(b), with its left side slightly affected by bend contours in the foil. The maximum phase difference across the core is 0.5π and we have tried to fit these data by means of the London model. Taking the London length λ_L^* as a free parameter, a value of 50 ± 5 nm has been obtained, as compared to the previous bulk value of 30 nm.

Values for the London depth in bulk specimens can be found in the literature, although it is important to remember that the most sensitive methods only measure changes of the penetration length with the temperature and not its absolute value.[16] Clem fit his bulk model[11] to neutron-diffraction data[9,12] to obtain 26.3 nm, whereas a value of 41 ± 4 nm resulted from polarized neutron reflectivity measurements.[17] It should be remarked that this latter value is one of the few absolute determinations of the superconducting penetration length in niobium and is in substantial agreement with earlier experimental and theoretical investigations.[17]

Considering that the hologram resolution is 20 nm, the question arises if the difference between previous values for λ_L and the present one is really significant. In typical holograms, the resolution of the reconstruction is about three times the carrier fringe spacing, and for the case of a pure phase object, the resolution may be improved to twice the spacing. While the levels of noise in the phase data increase commensurately with the resolution improvement, decreasing the resolution to values about $5-6\times$ the carrier fringes can suppress noise contributions.

For this reason we have investigated, using one-dimensional models,[10] the effect of the hologram resolution on the fitting of the phase. Our results indicate that the trends of the phase across the fluxon core are not significantly affected by the reconstruction resolution. Moreover, quantitative fits of the phase are possible even when the resolution is equal to λ_L, but with an error bar considerably lower than the point resolution, contrary to our expectations. Therefore, even at the highest hologram resolution of 20 nm, with an error of 5 nm, no overlap exists between our estimate and the previous ones. Whereas it cannot be excluded that in thin films the London length can take values larger than those obtained mostly from indirect measurements in bulk specimens,[9,17] more physical explanation is presented in the following. We show that the observed effects can be interpreted by extending our model to account for the influence of the specimen surfaces on the field lines.

THEORY

It should be recalled that the electron optical phase shift due to a fluxon depends mostly on the field topography at the specimen surfaces, as the main contribution is the external fringing field. In our previous calculations we assumed that the field at the surface is equal to that in the bulk and is constant within the film. This assumption is in contrast with the results of Hasegawa *et al.*[18] who, by solving numerically the Ginzburg-Landau equations for a thin superconducting film, have shown that when the field lines approach the surfaces they fan out so that the field width at the surface is larger than that in the bulk.

The numerical solution of the Ginzburg-Landau equations is decidedly nontrivial, especially considering that the data is the basis of subsequent calculations of the fluxon phase shift. Fortunately, Clem has also extended his model for the fluxon in a bulk specimen[11,12] to the thin film case taking into account the effects due to the finite thickness.[15] By using dimensionless quantities (e.g., lengths are measured in units of λ_L), he arrived at an analytical solution whose main features are briefly recalled below.

Let us consider a single vortex carrying the quantum of flux $\Phi_0=h/2e$ aligned along the z axis within the film of reduced thickness d centered on the (x,y) plane. Using reduced cylindrical coordinates (r,φ,z), Clem assumed that the order parameter within the film is not disturbed by the surface (this restriction has been recently removed by Fritz *et al.*[19] in their calculations of the field at the surface of a superconductor) and is described by the following function

$$\psi(r,\varphi,z)=\psi(r,\varphi)=f(r)\exp(i\varphi), \tag{2}$$

with

$$f(r)=\frac{r}{\sqrt{r^2+\xi_\nu^2}}, \tag{3}$$

where $\xi_\nu=\xi_c/\lambda_L$ is a reduced variational core parameter.

Hence, Clem looked for a solution for the φ component of the magnetic vector potential a_φ, which in the film obeys the second Ginzburg-Landau equation and in the vacuum the Laplace equation, given in reduced cylindrical coordinates by

$$\frac{\partial}{\partial r}\left(\frac{1}{r}\frac{\partial}{\partial r}[ra_\varphi]\right)+\frac{\partial^2}{\partial z^2}a_\varphi=\left(a_\varphi-\frac{1}{kr}\right)f^2 \tag{4}$$

and

$$\frac{\partial}{\partial r}\left(\frac{1}{r}\frac{\partial}{\partial r}[ra_\varphi]\right)+\frac{\partial^2}{\partial z^2}a_\varphi=0, \tag{5}$$

respectively, where $k=\lambda_L/\xi$ is the Ginzburg-Landau parameter.

The solution in the film can be written as the sum of two terms. The first, a particular solution of the inhomogeneous equation (4), is taken independent of z and is therefore identical with the Clem model for the bulk superconductor[11,12] given by

$$a_{\varphi b}(r)=\frac{1}{kr}\left(1-\frac{\sqrt{r^2+\xi_\nu^2}K_1(\sqrt{r^2+\xi_\nu^2})}{\xi_\nu K_1(\xi_\nu)}\right), \tag{6}$$

where K_1 is the first-order modified Bessel function of the second kind.

The second, $a_{\varphi s}(r,z)$, general solution of the homogeneous equation, is a surface correction term necessary to satisfy the boundary conditions. This term cannot be calculated analytically, unless a constant order parameter is assumed, i.e., $f=1$. This is a reasonable guess as the magnetic field varies over a larger length scale than the order parameter.

Therefore, using a method introduced by Pearl[20] of expanding the solution of the Ginzburg-Landau and Laplace equations into terms of their Hankel components, and taking into account the boundary conditions at the surfaces, infinity and the fluxon core, Clem arrived at the following solution for the magnetic vector potential $a_\varphi(r,z)$ in the whole space:

$$a_\varphi(r,z)=\frac{1}{k}\int_0^\infty J_1(qr)f_1(q)f_2(q)f_4(q)\exp[q(z+d/2)]dq \tag{7}$$

for $z<-d/2$ and

$$a_\varphi(r,z)=\frac{1}{k}\int_0^\infty J_1(qr)f_1(q)f_2(q)f_4(q)\times\exp[-q(z-d/2)]dq \tag{8}$$

for $z>d/2$ with

$$f_1(q)=\frac{1}{1+q^2}, \tag{9}$$

$$f_2(q)=[1+(q/Q)\coth(Qd/2)]^{-1}, \tag{10}$$

and

$$f_4(q)=[Q\xi_\nu K_1(Q\xi_\nu)]/[\xi_\nu K_1(\xi_\nu)], \tag{11}$$

where $Q=\sqrt{1+q^2}$.

Within the film, the vector potential is given by

$$a_\varphi(r,z)=a_{\varphi b}(r)+a_{\varphi s}(r,z), \tag{12}$$

with $a_{\varphi b}$ given by Eq. (6) or equivalently by

$$a_{\varphi b}(r)=\frac{1}{k}\int_0^\infty J_1(qr)f_1(q)f_4(q)dq \tag{13}$$

and

$$a_{\varphi s}(r,z)=-\frac{1}{k}\int_0^\infty J_1(qr)f_1(q)f_2(q)f_4(q)\times\frac{q\cosh(Qz)}{Q\sinh(Qd/2)}dq. \tag{14}$$

A useful way of representing the field distribution is to calculate from the previous equations the phase shift experienced by a coherent electron plane wave in an ideal experiment where the beam direction is parallel to the specimen surface (say to the y axis) and the apparent infinite thickness of the specimen is overlooked.[15] As the vector potential can be written in the form

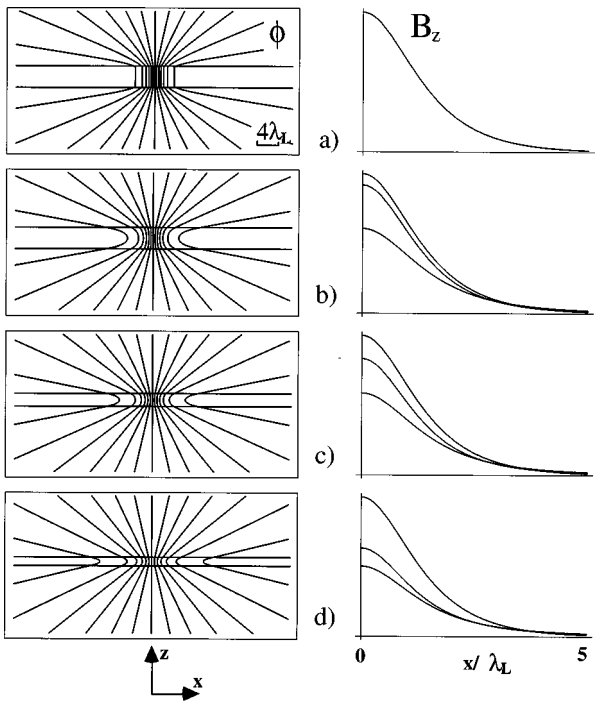

FIG. 2. In the left-hand column, projected phase maps of a fluxon's magnetic field calculated in a rectangle of reduced sides (λ_L units) of 40 and 20 for various reduced specimen thickness d. In (a), the bulk Clem model (no surface effects) for a reduced thickness of $d=3$; with surface effects $d=3$ (b); $d=2$ (c); $d=1$ (d). In the right-hand column, trends of the magnetic field B_z (arbitrary units) as a function of the radial distance for the cases (a)–(d). In each figure the upper curve is obtained using the bulk Clem model, the middle and lower curves refer to the value of B at the film center and at the film surface, respectively.

$$a_\varphi(r,z)=\frac{1}{k}\int_0^\infty J_1(qr)F(q,z)dq, \tag{15}$$

it turns out that the phase shift ϕ and the z component of the magnetic field B_z in the (x,z) plane are given by

$$\phi(x,z)=\int_0^\infty F(q,z)\frac{\sin qx}{q}dq \tag{16}$$

and

$$B_z(x,z)=\frac{\phi_0}{2\pi\lambda_L^2}\int_0^\infty F(q,z)qJ_0(qx)dq, \tag{17}$$

respectively.

RESULTS AND DISCUSSION

The left column of Fig. 2 reports fluxon phase maps $\phi(x,z)$ (giving a good indication of the projected magnetic field distribution) calculated in a rectangle with reduced sides of 40 and 20 for reduced specimen thicknesses of $d=3$ (a and b), $d=2$ (c), and $d=1$ (d). In the right column are drawn (in arbitrary units) the trends of the z component of the magnetic field calculated up to a reduced distance from the core of 5 at the film surface (lower curves), at the film center (intermediate curves) and, for reference, the bulk Clem model (upper curves).

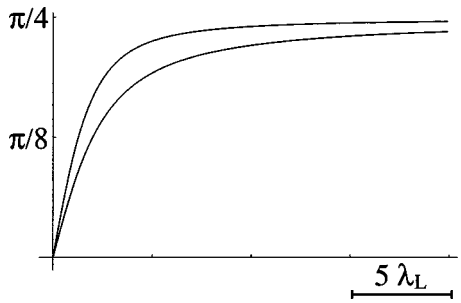

FIG. 3. Trends of the phase calculated for a specimen of thickness $d=2\lambda_L$ tilted at 45°. The upper curve refers to the total field and the lower curve is related to the external field alone, calculated for a flux tube of negligible length. While there are differences due to flux tube length near the core, the major contribution to the phase shift is the external fringing field.

These curves obviously coincide for the case (a) relative to the straight flux tube model, whereas the dependence of the two-dimensional projected field distribution and its z component on the specimen thickness can be better appreciated by (b)–(d). In particular, whereas at $d=3$ (b) the field at the specimen center is nearly equal to the bulk value, it diminishes with decreasing thickness becoming nearly equal to the surface field at $d=1$ (d). Also the surface field diminishes with decreasing thickness but in a less marked way, its maximum value always being about one half of the bulk value.

These figures from our analytic model agree well with the corresponding ones of Hasegawa *et al.*[18] calculated by means of the more arduous numerical solution of the Ginzburg-Landau equations. If we insert into our equations data from that paper (considering a fluxon viewed edge-on rather than the tilted case), very good agreement is obtained. Moreover, absent from our model are the bending of the flux lines caused by the periodic boundary conditions assumed in the numerical calculations.[18] The plots of the field distribution profiles also show good agreement, with only a small difference at the core. This is to be expected in the core region as the assumption of constant order parameter $f=1$ breaks down. An additional advantage of the analytical model, with respect to the numerical solution, is that it can be easily adapted for calculating the electron optical phase shift in the tilted specimen geometry of transmission electron microscopy experiments.

In order to compare the new model with the earlier results, let us first recall that the phase shift was calculated by convoluting the analytical phase of the straight flux tube[2,8] with the z component of the magnetic-field distribution. If the magnetic field at the surface given by Eq. (16) is inserted, then the phase-shift profile across the fluxon shown in the upper curve of Fig. 3 is obtained, calculated for a specimen of thickness $d=2\lambda_L$ tilted at 45°. It should be noted that we have implicitly assumed that the field within the specimen is constant and equal to that at the surface. It will be shown later that this assumption, which considerably simplifies the calculations, has a negligible effect on the final result.

The lower curve in Fig. 3 reports the phase shift calculated with the same surface magnetic field, but by taking a flux tube of negligible length. In this way it is possible to disentangle the effects on the phase shift of the external and internal fields. While it can be ascertained that the main contribution to the phase is due to the external field, nonetheless the qualitative behavior of the two curves is rather different. In particular, for the lower curve, it should be noted that the maximum phase difference is lower than the expected limiting value of $\pi/4$, which is reached only at very large distance from the core, about one order of magnitude larger with respect to total field case (upper curve). Moreover, if these phase profiles are analyzed according the previous procedure, by fitting them with the London phase in Eq. (1), over a reduced distance from the fluxon core ranging between 10 and 50, then rather different results are obtained.

For the upper phase (total field) the ratio between λ_L^*/λ_L ranges between 1.73 and 1.88 (i.e., by taking $\lambda_L=30$ nm between 52 and 57 nm), whereas for the external field alone (lower curve) this variation is much higher, between 2.38 and 3.12 (i.e., between 72 and 96 nm, respectively). Therefore, whereas the values obtained for the total field are in good agreement with the experimental value, the fit procedure is more troublesome when applied to the external field alone, and this should be attributed to the previously noted different asymptotic approach to the limiting value of $\pi/4$.

Another fitting approach, relying on the similar trend of the magnetic fields in Fig. 2, is to approximate the field at the surface and at the center by means of the bulk Clem model with the same value of the parameter k but with a suitably chosen London penetration depth λ_L^c. Further, we take into account that the total flux across any section of the specimen should be constant and equal to Φ_o. If the field is well described by a suitably rescaled Clem model, it turns out that the broadening of the field, given by the ratio $s=\lambda_L^c/\lambda_L$, is also equal to the inverse square root of the ratio of the maximum field values at the core.

Considering the case $d=2$ it turns out that at the surface $s=1.304$. If a best fit procedure is adopted, instead of the ratio between maxima, the slightly different value of $s=1.345$ is obtained. From these data the one-dimensional phase shift across the fluxon at the surface can be calculated.[10] It turns out that the curves obtained from the two values of s differ by a maximum error of 0.02 rad, i.e., are experimentally indistinguishable as the present state of the art phase measurements by holographic methods[7] have a limiting accuracy of the order of $0.06\ \text{rad}\simeq 2\pi/100$.

When this phase is fit with the London model, as in Fig. 1, the value of the penetration depth giving the best fit λ_L^*, again amounts to 52 nm, in agreement with previous results. The agreement between different fitting procedures confirms that, in spite of the shortcomings previously noted, thickness effects do cause a broadening of the magnetic field with respect to the bulk case.

Finally, let us consider the effect of flux tube bending within the film, evident from the first column of Fig. 2. This raised the question of how this bending influences the phase shift in the tilted specimen geometry, since the straight flux tubes considered in our first model are now substituted by deformed flux tubes, with the deformation dependent on the coordinates in the specimen plane. A detrimental consequence of this fact from the computational point of view is that the phase shift can no longer be calculated by convolution.

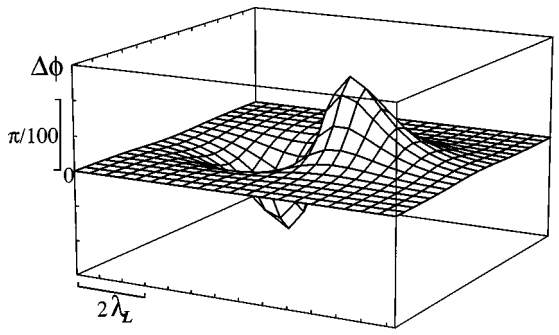

FIG. 4. Map of the phase difference due to the deformation of flux tubes for a reduced specimen thickness of $d=2$. The maximum error is of the order of $\pi/100$ and is therefore negligible in the calculation of the phase shift.

While the bending effect is expected to be small, since the main contribution to the phase shift is the external field linked to the field topography at the surface,[2,8] we have tried to obtain a quantitative estimate of it by assuming that the field in the specimen is still described by a bulk Clem model with λ_L^c depending on the z coordinate. Moreover, we approximated this dependence by a parabolic trend that is therefore determined by its values at the surface and at the specimen center, see Fig. 2.

We consider that the external field depends only on the positions of the entry and exit poles and is decoupled from the shape of the flux tube within the specimen. Thus, it turns out that the phase difference between the two models depends on the internal field alone and can be calculated with less trouble than the total phase shift. Figure 4 reports the map of the phase difference for the case $d=2$. It can be ascertained that the maximum error associated with the bending of flux tubes is again of the order of $\pi/100$ and can be safely neglected. Similar calculations carried out for the cases $d=3$ and $d=1$ show that the maximum error is 0.06 and 0.013 rad, respectively.

CONCLUSIONS

We have quantitatively measured the London penetration depth of superconducting vortices from high-resolution holographic phase data by assuming a bulk London model for the magnetic field topography and by fitting the phase across the core with a one-dimensional London model. The discrepancy of the obtained value of 50 nm for the penetration depth with those resulting from other measurements has been explained by taking into account thickness effects. If these effects are properly considered and the theoretical model correspondingly improved, it turns out that the specimen thickness strongly influences the measured phase shift, the images of superconducting vortices obtained by electron microscopy and holography techniques and hence the extraction of reliable quantitative estimates of parameters such as the London penetration depth. These results demonstrate the importance of the assumed model in the analysis of the experimental data. We have shown that the above value of 50 nm is consistent with the commonly accepted value of 30 nm as well as with the other experimental values for the London penetration depth. Moreover, it has been shown that the flux tube bending within the specimen can be overlooked within the present state of the art precision in the phase measurement. Thus the straight flux tube model with its associated computing benefits can be safely applied, either in combination with a field surface model or with a bulk London model characterized by a larger phenomenological penetration depth.

ACKNOWLEDGMENT

The authors would like to acknowledge Professor J. R. Clem for sharing the results of his research.

[1] K. Harada, T. Matsuda, J. Bonevich, M. Igarashi, S. Kondo, G. Pozzi, U. Kawabe, and A. Tonomura, Nature (London) **360**, 51 (1992).
[2] J. E. Bonevich, K. Harada, H. Kasai, T. Matsuda, T. Yoshida, G. Pozzi, and A. Tonomura, Phys. Rev. B **49**, 6800 (1994).
[3] K. Harada, T. Matsuda, H. Kasai, J. E. Bonevich, T. Yoshida, U. Kawabe, and A. Tonomura, Phys. Rev. Lett. **71**, 3371 (1993).
[4] J. E. Bonevich, K. Harada, H. Kasai, T. Matsuda, T. Yoshida, G. Pozzi, and A. Tonomura, Phys. Rev. Lett. **70**, 2952 (1993).
[5] G. F. Missiroli, G. Pozzi, and U. Valdrè, J. Phys. E **14**, 649 (1981).
[6] A. Tonomura, Adv. Phys. **41**, 59 (1992).
[7] A. Tonomura, *Electron Holography* (Springer, Berlin, 1993).
[8] A. Migliori, G. Pozzi, and A. Tonomura, Ultramicroscopy **49**, 87 (1993).
[9] R. P. Huebener, *Magnetic Flux Structures in Superconductors* (Springer, Berlin, 1979).
[10] G. Pozzi, J. E. Bonevich, K. Harada, H. Kasai, T. Matsuda, T. Yoshida, and A. Tonomura, Microsc. Microanal. Microstruct. **6**, 559 (1995).
[11] J. R. Clem, J. Low Temp. Phys. **18**, 427 (1975).
[12] J. R. Clem, in *Low Temperature Physics-LT14*, edited by M. Krusius and M. Vuorio (North-Holland, Amsterdam, 1975), Vol. 2, p. 285.
[13] G. Pozzi, J. E. Bonevich, K. Harada, H. Kasai, T. Matsuda, T. Yoshida, and A. Tonomura, in *Electron Holography*, edited by A. Tonomura *et al.* (Elsevier, Amsterdam, 1995), p. 125.
[14] J. E. Bonevich, K. Harada, H. Kasai, T. Matsuda, T. Yoshida, and A. Tonomura, Phys. Rev. B **50**, 567 (1994).
[15] J. R. Clem, in *Inhomogeneous Superconductors*, edited by D. U. Gubser *et al.*, AIP Conf. Proc. No. 58 (AIP, New York, 1979), p. 245.
[16] M. Tinkham, *Introduction to Superconductivity*, 2nd ed. (McGraw-Hill, New York, 1996).
[17] G. P. Felcher, R. T. Kampwirth, K. E. Gray, and R. Felici, Phys. Rev. Lett. **52**, 1539 (1984).
[18] S. Hasegawa, T. Matsuda, J. Endo, N. Osakabe, M. Igarashi, T. Kobayashi, M. Naito, A. Tonomura, and R. Aoki, Phys. Rev. B **43**, 7631 (1991).
[19] O. Fritz, M. Wülfert, H. J. Hug, H. Thomas, and H.-J. Güntherodt, Phys. Rev. B **47**, 384 (1993).
[20] J. Pearl, J. Appl. Phys. **37**, 4139 (1966).